13B.4

EVOLUTION OF A WINTERTIME PACIFIC NORTHWEST MINI-SUPERCELL AND TORNADO

David Elson*, Jonathan Wolfe, Charles Dalton, William R. Schneider
NOAA/National Weather Service Forecast Office
Portland, Oregon

1. INTRODUCTION

On 10 January 2008, a rare mini-supercell developed over southwest Washington, producing a series of tornado touchdowns along a 19 km track in Clark County, Washington. The first touchdown likely occurred on the western shore of Vancouver Lake, while the first significant damage occurred on the east side of the lake (Figure 1), where the tornado destroyed a boathouse full of sculling equipment. The tornado went on to damage over 200 trees, some of which were more than 1 meter in diameter. Thirty to forty homes were damaged, and the tornado tipped over a parked semi-trailer as it trekked across Clark County. The extended lifetime and track length of this EF-1 tornado made it the most damaging to occur in the region in 35 years.

The close proximity of the storm to the KRTX Weather Surveillance Radar gave meteorologists an unusual opportunity to analyze the development of a Pacific Northwest supercell thunderstorm and tornado. In addition to radar data, an examination of satellite data and the pre-storm environment yielded some clues as to the reasons for this storm's severity as compared to other storms that have occurred in the region.

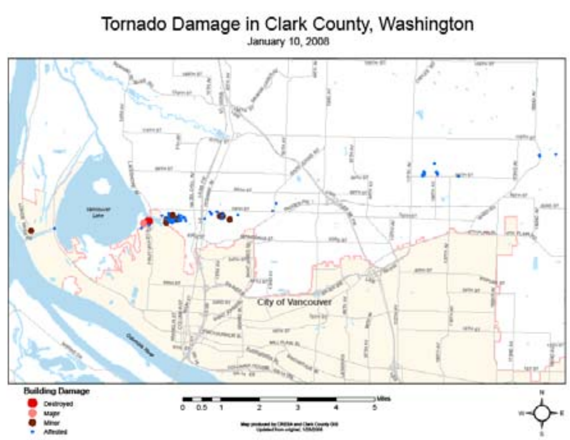

Figure 1. Damage map for Clark County, Washington. Map courtesy of CRESA and Clark County Washington GIS.

Corresponding author address: David B. Elson, National Weather Service, 5241 NE 122nd Ave.., Portland, OR 97230; e-mail dave.elson@noaa.gov

2. PACIFIC NORTHWEST THUNDERSTORM CLIMATOLOGY

The Pacific Northwest is not typically known for severe convective weather, especially west of the Cascade Mountains. Most severe weather reported in this region is non-convective, and occurs during the fall and winter months. Occasionally though, conditions conducive to development of severe thunderstorms and tornadoes do evolve. Such was the case with the January 2008 tornado that swept across Vancouver, Washington.

The National Weather Service Forecast Office in Portland, Oregon, serves a county warning area (CWA) comprised of southwest Washington and northwest Oregon. This area averages about one tornado per year, based on reports from 1950 through 2008. Nationally, most observed tornadoes are weak. Approximately 77% of reported tornadoes receive a rating of F0 to F1 (National Climatic Data Center, 2008). Strong tornadoes, rated F2 to F3 account for another 22% of tornadoes. Violent tornadoes, rated F4 to F5, make up only about 1% of observed tornadoes. The bias towards weak tornadoes is more pronounced in the Portland CWA; no tornado in the Portland CWA has received a rating above F3, and only two were of F2 or F3 strength. The remaining 58 tornadoes all received a rating of F0 or F1.

Tornadoes occurring in the Portland CWA favor the low elevations; tornadoes have been observed along the coast and in the Willamette Valley. Few reports have been received from areas of mountainous terrain (Figure 2). While the geographic signal for distribution of tornadoes appears weak, two of the three most significant tornadoes recorded in the Portland CWA developed within a few miles of each other in western Clark County, Washington. Topographic influences on wind are likely contributors to the subject tornado as well as the 5 April 1972 Vancouver tornado.

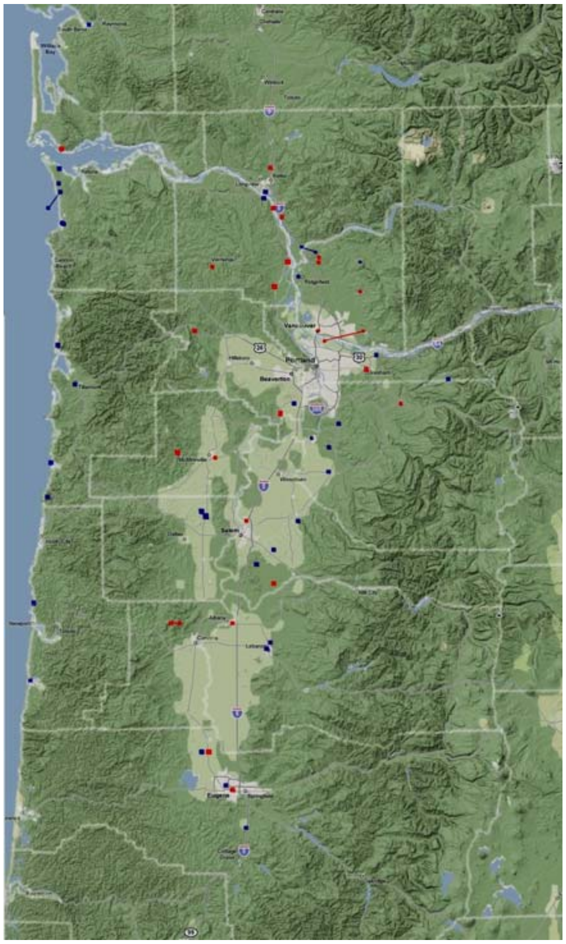

Figure 2.Locations of all recorded tornadoes from 1950 to 2007, within the NWS Portland, OR Forecast Area. In this image, the Willamette Valley runs north to south through the center of the image, and is represented by the pale green topography. Blue dots represent cool season (September through February) tornadoes, and red dots represent warm season (March through August) tornadoes. Tornado Data from the NCDC Storm Data.

Seasonally, there is a distinct bimodal distribution of tornado occurrence in the Pacific Northwest (Figure 3). A maximum in convective activity is associated with the spring and summer months, as is the case east of the Rocky Mountains. A second maximum in Northwest tornadoes falls from October through December.

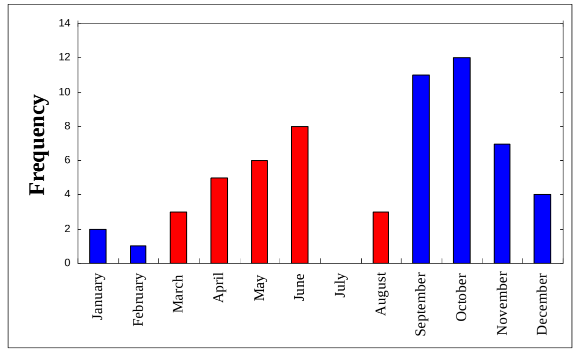

Figure 3: Seasonal distribution of tornadoes for the Portland National Weather Service CWA for 1950-2008. Warm season tornadoes are in red, cool season tornadoes in blue.

Two synoptic patterns are locally recognized for producing severe convective weather in Portland's CWA. The first, more common pattern, occurs during the spring and summer convective season, and involves an upper level cutoff low off the northern California coast. The weakly sheared, dry environment supports mostly elevated, single cell storms, at times producing downbursts and hail. The 10 January 2008 tornado synoptic pattern falls in a second regime. This regime is more frequent in fall and winter months, and involves the approach or passage, of an upper level trough. This pattern is similar to one identified by Hales (1994). Tornadoes in California, and the 5 April 1972 Vancouver Washington tornado, occurred most frequently under strong cyclonic circulation, both at the surface and aloft (Figure 4). The region of tornadogenesis was located on the cyclonic side of a strong polar jet, under mid level cold advection, with an onshore flow of moist Pacific air. This frequently occurs in a post-frontal air mass.

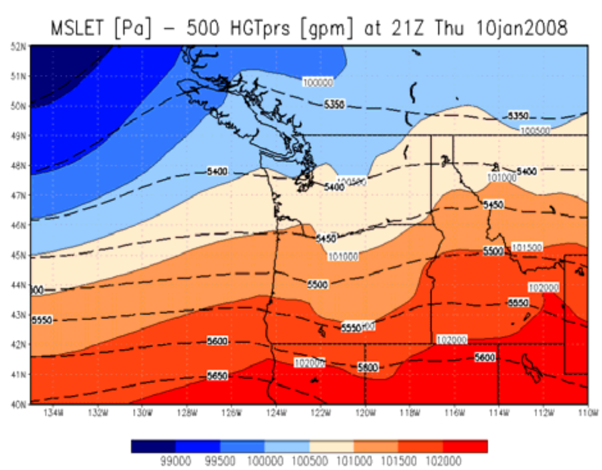

Figure 4. North American Reanalysis of 500mb heights (dashed lines) and MSLP (solid lines and fill) for 21z on January 10, 2008.

The interaction of post-frontal showers and channeled surface winds through the Willamette Valley is beneficial to the development of a tornadic storm. In the post-frontal environment, surface pressure gradients interact with topography to induce a south wind in the Willamette Valley, and a southeast wind in the lower Columbia River Valley. Climatological tendencies of wind in the confluence of the Willamette and Columbia River Valleys can be seen in an annual wind rose plot for Portland International Airport (Figure 5). As showers move off of the higher terrain of the coast range, they tend to encounter backed surface winds throughout the valley, enhancing low level vertical wind shear.

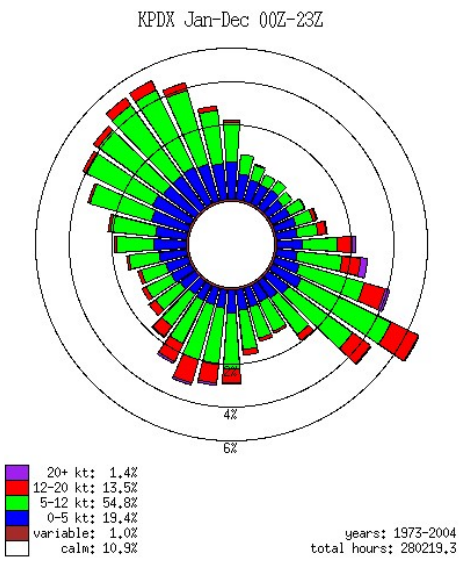

Figure 5. Wind rose for Portland International Airport.

3. PRE-STORM ENVIRONMENT

The synoptic pattern on 10 January 2008 was not that unusual for the time of year. An upper level trough sagged southward over the CWA. Cold air advection aloft over a post-frontal air mass generated the instability necessary for the storm to develop.

The pre-frontal, 1200 UTC sounding from Salem, Oregon (KSLE), shows a stable atmosphere with a veering wind profile (Figure 6). Both speed and directional shear were present with much of the directional shear occurring between the surface and 900 hPa. Strong westerly flow aloft indicated the presence of an upper level jet moving over the Pacific Northwest. A vorticity maximum, analyzed as $30 \cdot 10^{-5}$ s^{-1} by the 1800 UTC NAM model, moved across the northern Willamette Valley around 2100 UTC. The atmosphere was generally moist, with a mid-level dry layer.

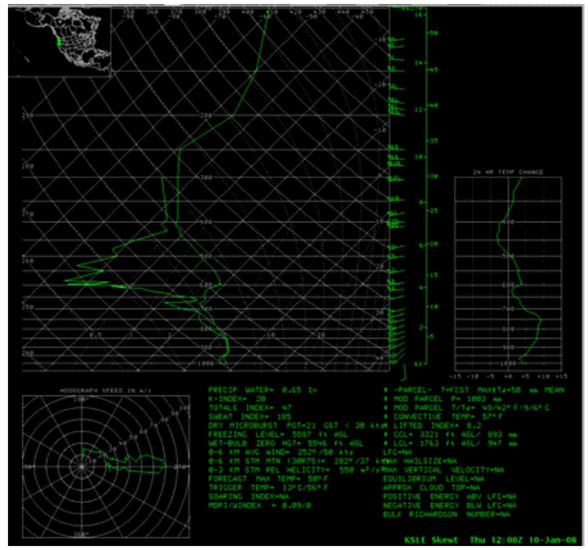

Figure 6. 1200 UTC 10 January 2008 KSLE (Salem, OR) sounding and hodograph.

During the morning, the northern Willamette Valley experienced rapid heating as cloud cover dispersed. Observed temperature and dew point values for Vancouver, WA (KVUO) at 2000 UTC departed from the model forecast by +2 °C (+4 °F) and -2 °C (-3 °F), respectively. This deviation resulted in a much more unstable atmosphere than was anticipated from the model forecast. Modifications to the 2000 UTC NAM BUFR sounding with 2000 UTC observed surface temperature and dew point from KVUO produced a CAPE of 700 J kg^{-1} versus the 200 J kg^{-1} forecast by the model. Additionally, the expected cloud top increased from 7.3 km (24 kft) to 9.4 km (31 kft), the lifted indices dropped from +2 to -2, and the equilibrium level increased from 4.6 km (15 kft) to 6.7 km (22 kft).

Modifying the 2000 UTC NAM BUFR hodograph with the south wind observation from KVUO increased the 0-3 km storm relative helicity from 168 to 182 $m^2 s^{-2}$. However, a more complicated wind profile existed around the area. Prior to the storm reaching Vancouver at 1900 UTC (Figure 7), surface winds were southerly in the Willamette Valley, southwesterly in the Coast Range, and southeasterly along the Columbia River. As such, the modifications to the hodograph may have underestimated the increase in the 0-3 km storm relative helicity value.

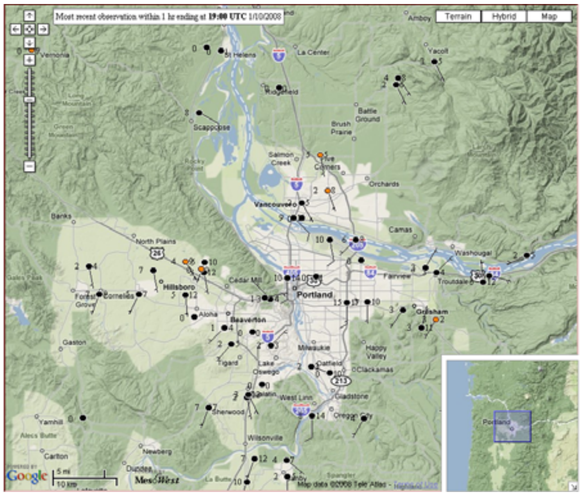

Figure 7. Surface wind plot for the Portland-Vancouver area at 1900 UTC 10 January 2008.

Figure 8 shows a velocity image from the 1853 UTC 10 January 2008 KRTX radar, showing the presence of Horizontal Convective Rolls (HCRs) in the pre-storm boundary layer. The white line indicates the orientation of the rolls. The HCRs were also apparent in visible satellite imagery that morning (Figure 9). The HCRs persisted throughout the morning and early afternoon, before the developing storm disrupted them. HCRs have been shown to favorably modify an otherwise stable environment into one that supports the development of supercells and tornadoes (Wilson et al., 1992). The HCRs were oriented parallel to the mean wind in the upper boundary layer around 1500 m AGL and along the eventual tornado track. Reflectivity and velocity radar data from KRTX show roll-to-roll separation of approximately 5 km, with horizontal shear of around 20 kts. The HCRs likely played a critical role in the development of the mesocyclone and subsequent tornado by providing a source of horizontal vorticity which was incorporated into the storm updraft.

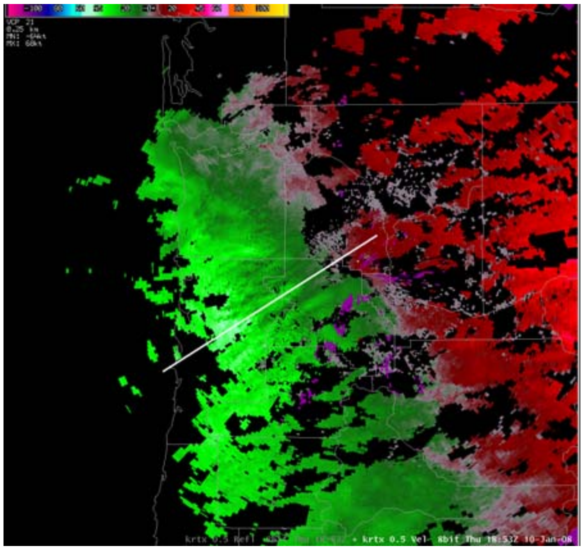

Figure 8. 1853 UTC 10 January 2008 velocity imagery from the KRTX (Portland, OR) radar at the time when the convective cluster that spawned the Vancouver tornado was just moving ashore. HCR's are illuminated by linear striations of the incoming echoes and their orientation is indicated by the white line.

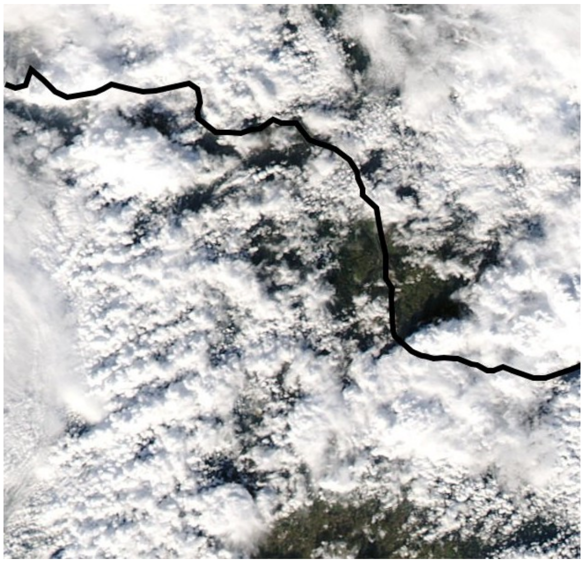

Figure 9. 1925 UTC January 2008 MODIS visible satellite imagery for the northwest corner of Oregon and the southwest corner of Washington. The black line represents the Columbia River.

4. STORM EVOLUTION

4.1 *Storm Initiation*

The short wave that produced the Vancouver tornado originated in an area of strong positive vorticity advection. A comma cloud appeared on IR satellite imagery (Figure 10) about 185 km off the Oregon coast as early as 1615UTC. As the comma cloud moved onshore and over the HCRs, it rapidly intensified, disrupting the convective rolls.

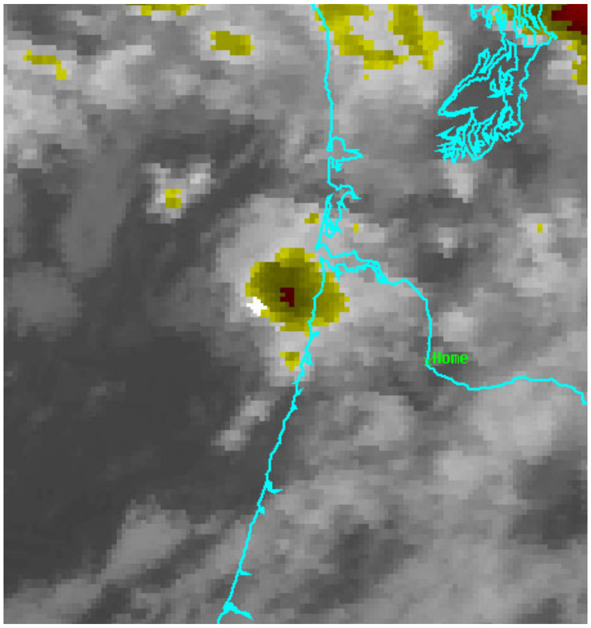

Figure 10. Infrared satellite picture at 1800 UTC showing comma cloud approaching the North Oregon Coast. Outlines of western Oregon and Washington are shown in blue.

The rapid convective development that ensued was somewhat masked by the proximity of the storm to the radar's cone of silence. As the storm emerged from the radar's cone of silence at 1951 UTC, velocity data indicated enhanced low level inflow feeding into the south side of the storm. Further intensification may have benefited from the conservation of potential vorticity as it moved east of the Tualatin Mountains (elevation ~400 m) and over the Willamette Valley floor, which drops to near sea level in only 4 km.

4.2 *Development of the Tornado and Mini-Supercell*

At 2002 UTC, low level radar velocity data (Figure 11) suggest the presence of a downburst as the storm crossed the Tualatin Mountains and approached the Columbia River Valley. Evident in storm relative velocity, a weak notch on the leading edge of the gust front coincides with the axis of the convective roll along which the storm formed. This hints at the first signs of low level rotation preceding the initial tornado development, strongly suggesting that the convective roll was significant in the tornado's development. Weak rotational velocities (Vr) of up to 8 m/s (15 kts) appeared in the mid levels (2.0 km or 6.7 kft AGL) of the storm at this time, with 26 m/s (50 kts) of divergence near the storm top at 7.6 km (25 kft). Concurrent reflectivity data (Figure 12) showed the storm oriented as a short convective line, with a slight leaning of the storm tops downwind (possibly the result of the time lag in sampling higher elevation slices).

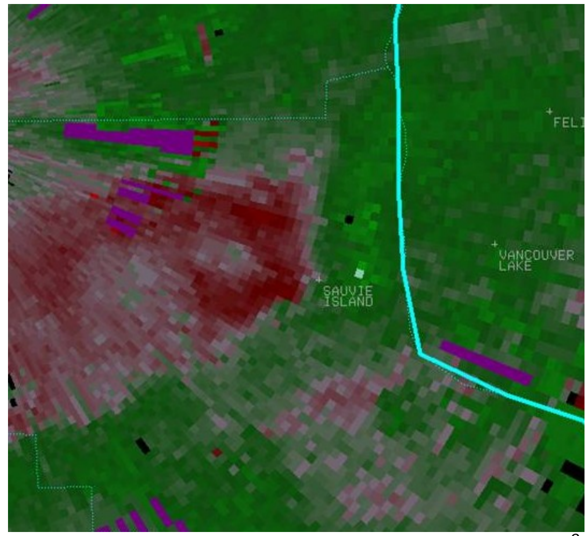

Figure 11. Storm relative motion at 2002 UTC, at 0.5^o at a range of 13 km (7 nm) from the radar. The red crescent of outbound velocities is suggestive of a downburst, while a notch on the forward edge of the downburst nearing Sauvie Island (near center of image) suggests a small scale rotation. The light blue line through the right half of the image represents the Columbia River near Vancouver Washington.

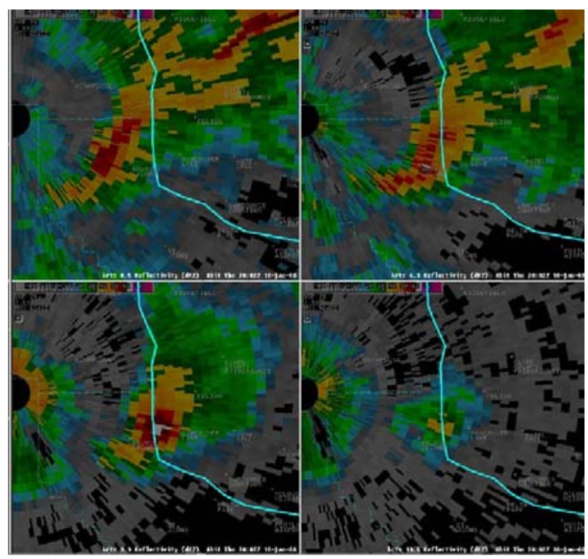

Figure 12. Reflectivity data at 2002 UTC. Upper left image is at 0.5^o, upper right is 4.3^o, lower left is 9.9^o, and lower right is 19.5^o.

By 2008 UTC, a weak mesocyclone and a tornado vortex signature developed simultaneously. Over the next half hour, the mesocyclone was centered around 2.1 km (7.0 kft) above ground level (AGL), with the highest resolvable rotation around 4.6 km (15.0 kft). Rotational speeds in the mesocyclone were fairly consistent from 2008 UTC and 2047 UTC, ranging between 11 and 14 m/s (21 and 27 kts). The diameter of the rotating core was generally 5.6 km (3.0 nm) or less in that time period. Also evident was that the tornadic storm's motion deviated to the right of the track of other showers and storms that day, which favorably enhanced the low level helicity by increasing storm inflow.

The tornado vortex signature at the lowest elevation slice of 0.5^o between 600 and 800 m (1.9 and 2.5 kft) AGL intensified quickly. Vr reached 15 m/s (30 kts) by 2002 UTC, and peaked at 35 m/s (68 kts) by 2014 UTC (Figure 13). Gate-to-gate Vr maintained values around 15 m/s through 2037 UTC. Reflectivity data from that period (Figure 14) showed classic signatures of tornado-producing supercells (Lemon and Doswell, 1979). These signatures included a low level hook echo, and a weak echo region (WER). The tornado vortex signature and mesocyclone correlated well with tornado reports, which began at 2015 UTC and ended at 2040 UTC.

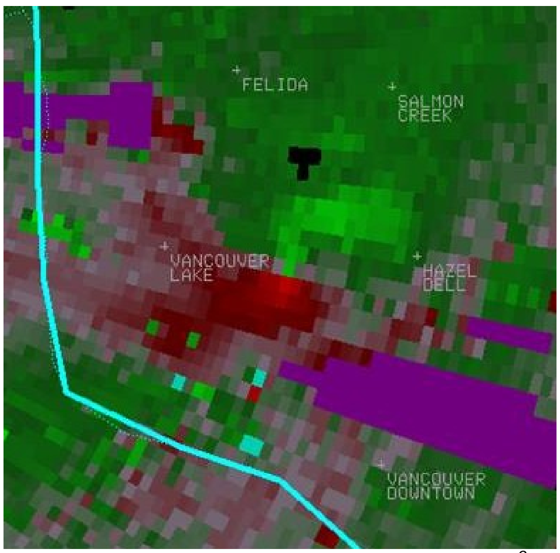

Figure 13. Storm relative motion at 2014 UTC, at 0.5^o at a range of 22 km (12 nm) from the radar.

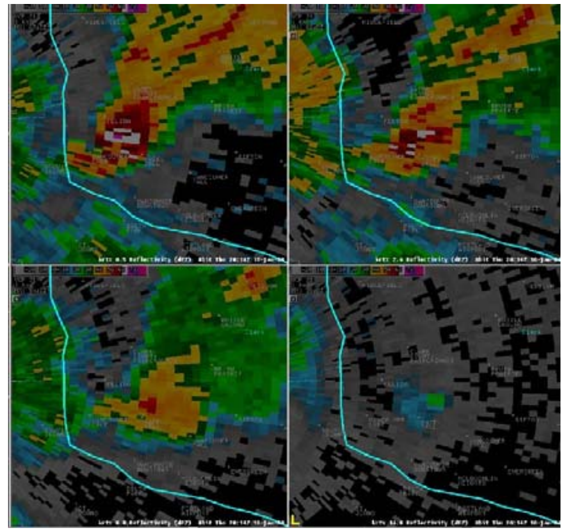

Figure 14. Reflectivity data at 2014 UTC. Upper left image is at 0.5^o, upper right is 2.4^o, lower left is 6.0^o, and lower right is 14.0^o.

Several potentially significant sources for rotation as discussed earlier in the pre-storm environment section, came into play when the storm crossed the Columbia River. Vertical stretching resulted from both storm intensification and from the storm moving out into lower terrain of the Columbia River Valley. A second mechanism for rotation was the interaction of the outflow boundary with an HCR (Figures 15 and 16). As the outflow boundary undercut the convective roll normal to its axis, the convective roll was lifted and tilted vertically. The importance of a preexisting surface boundary in enhancing tornado development has been discussed in a variety of other case studies, including Brady and Szoke (1989), Golden and Sabones (1991), Elson (1996), Schmocker et al. (2000), Suzuki et al. (2000), and Crosbie and Wolf (2002). Finally, low level helicity increased as inflow backed to the southeast when the storm moved into the Columbia River Valley.

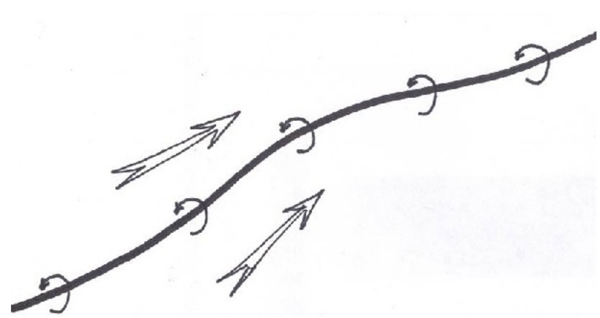

Figure 15. Schematic diagram of ambient low level flow (open arrows) with a horizontal convective roll (heavy black line with arrows)

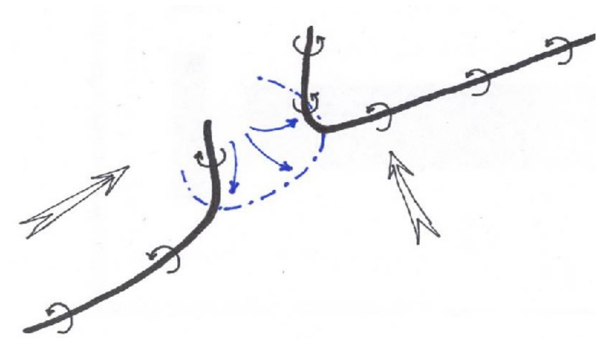

Figure 16. Schematic diagram of the horizontal convective roll undercut by an outflow boundary (blue dashed line with arrows). Ambient low level flow to the south of the boundary had backed as the storm moved into the Columbia River Valley.

The storm met the single distinguishing characteristic of a supercell by developing a persistent and deep mesocyclone, as defined by Doswell and Burgess (1993). Dimensions of the storm compared favorably with those classified by Grant and Prentice (1996) as a mini supercell. The lowest altitude diameter of the mesocyclone remained 3.7 km (2 nm) or less throughout its life cycle. The tightest low altitude diameter occurred just prior to the first tornado report, at the same time when gate to gate Vr peaked at 35.0 m/s (68 kts). The mesocyclone aloft was best defined between 1.9 and 2.3 km (6.2 and 7.7 kft) AGL. The top of the mesocyclone averaged around 4.3 km (14.0 kft) AGL, maintaining an average depth deeper than most mesocyclones in mini supercells. Storm tops, as defined by the maximum height of 20 dBZ reflectivity, averaged around 7.3 km (24 kft).

4.3 *Storm Decay*

By 2047 UTC, the storm began to move into the Cascade Mountains. The terrain disrupted the low level wind field, and colder air, enhanced by snow cover, reduced buoyancy. The storm weakened rapidly.

5. SUMMARY

Tornadoes and supercells are a rarity in the Pacific Northwest. The southwest Washington tornado of 10 January 2008 was one of the most significant tornadoes in the area in the past 35 years. The storm developed in a weather regime similar to that of prior tornadoes in the region, under a cold core trough aloft with a low level marine air mass.

As with most storms in the Pacific Northwest, buoyancy was modest when compared to severe thunderstorms in the eastern half of the United States. The mini-supercell developed in an area with several factors that contributed to a favorable vertical wind shear profile. Local topography helped to both enhance the shear profile and intensify existing storm circulation through channeled low level flow and vertical stretching. Probably the most significant source of vorticity came through the ingestion of a HCR. The simultaneous development of a rotating mesocyclone and the tornado vortex suggests the tornado spun up from low level influences, while the deep mesocyclone played a role in the longevity of the storm and tornadoes.

6. ACKNOWLEDGEMENTS

The authors wish to acknowledge Julia Ruthford for her help in preparing images, and Kirsten Elson for her help with editing.

7. REFERENCES

Brady, R. H., and E. J. Szoke, 1989: A case study of nonmescocyclone tornado development in Northeast Colorado: Similarities to waterspout formation. *Mon. Wea. Rev*., **117,** 843-856.

Crosbie, C., and R. Wolf, 2002: WSR-88D observations of non-descending tornadogenesis in proximity to a synoptic scale frontal boundary: A case study of 18 May 2000 in Northern Illinois. Preprints, 21st Conf. on Severe Local Storms, San Antonio, TX, Amer. Meteor. Soc.

Doswell, C. A. III, and D. W. Burgess, 1993: Tornadoes and tornadic storms: A review of conceptual models. *The Tornado: Its Structure, Dynamics, Prediction and Hazards* (Geophys. Monogram. 79), C. Church, Ed., Amer. Geophys. Union, 161-172.

Elson, D. B., 1996: On the role of outflow boundary interactions with bow echoes in the development of non-supercell tornadoes. *Preprints*, *18th Conf. on Severe Local Storms,* San Francisco, CA, Amer. Meteor. Soc., 751-755.

Golden, J. H., and M. E. Sabones, 1991: Tornadic waterspout formation near intersecting boundaries. *Preprints, 25th Int. Conf. on Radar Meteorology,* Paris, France, Amer. Meteor. Soc., 420–423.

Grant, B. and R. Prentice, 1996: Mesocyclone characteristics of mini supercell thunderstorms. *Preprints, 15th Conf. on Wea. Anal. and Forecasting*, Norfolk, Virginia, Amer. Meteor. Soc., 362-365.

Hales, J. E., 1994: The Vancouver WA tornado on April 5, 1972 as a benchmark for west coast significant tornado episodes. *Preprints, Sixth Conf. on Mesoscale Processes*, Portland, Oregon, Amer. Meteor. Soc., 134-137.

Lemon, L. R., and C. A. Doswell III, 1979: Severe thunderstorm evolution and mesocyclone structure as related to tornadogenesis. *Mon. Wea. Rev*., **107**, 1184-1197.

National Climatic Data Center. 10 April 2008. NOAA/National Climatic Data Center. 17 October 2008. <http://www.ncdc.noaa.gov/oa/climate/severeweather/tornadoes.html>.

Schmocker, G. K., R. W. Przybylinski, and E. N. Rasmussen, 2000: The severe bow echo event of 14 June 1998 over the mid-Mississippi valley region: A case of vortex development near the intersection of a preexisting boundary and a convective line. *Preprints, 20th Conf. on Severe Local Storms,* Orlando, FL, Amer. Meteor. Soc., 169-172.

Suzuki, O., H. Nilno, H. Ohno, N. Nirasawa, 2000: Tornado producing mini supercells associated with Typhoon 9019. *Mon. Wea. Rev.,* 128, 1868-1881.

Wilson, J.W., G.B. Foote, N.A. Crook, J.C. Fankhauser, C.G. Wade, J.D. Tuttle, C.K. Mueller, and S.K. Krueger, 1992: The Role of Boundary-Layer Convergence Zones and Horizontal Rolls in the Initiation of Thunderstorms: A Case Study. *Mon. Wea. Rev.*, **120**, 1785–1815.